

NSM FRP Shear Strengthening of RC Beams with Internal Stirrups

Pongsak Wiwatrojanagul¹, Borvorn Israngkura Na Ayudhya² and Raktipong Sahamitmongkol³

¹ Asian Institute of Technology, Thailand.

² Department of Civil Engineering, Rajamangala University of Technology Krungthep.

³ Construction and Maintenance Technology Research Center, Sirindhorn International Institute of Technology, Thammasat University.

Correspondence:

Pongsak Wiwatrojanagul
Asian Institute of Technology, Thailand.
Email: wiwatrojanagul@gmail.com

Abstract

This article presents an experimental study on shear strengthening of reinforced concrete (RC) by near-surface mounted (NSM) fiber reinforced polymer (FRP) rods, comparing the experimental results with three existing formulations for the NSM FRP shear strengthening technique. The NSM FRP technique is done by making a groove in concrete cover, putting FRP rods in the groove, and fixing them with epoxy adhesive. To evaluate the efficiency of NSM FRP strengthening, two experiments were conducted. In the first experiment, bond testing in pull-out conditions was conducted to compare a suitability of different groove sizes (1.5 and 2.0 times of rod diameter) for NSM FRP application. In the second experiment, strengthened beams with stirrups were tested to evaluate influences of key parameters on shear capacity and failure mode. Three examined parameters used in such testing were two types of FRP (Carbon and Aramid), spacing between the rods and slope of FRP rods. Peeling-off failures of NSM layers was found in some cases. This failure mode limited the efficiency of NSM FRP technique.

Keywords: peeling-off, shear, strength, concrete, reinforce, near-surface mounted

1. Introduction

Strengthening of existing reinforced concrete (RC) structures has become an important activity in structural engineering. Main reasons for strengthening a structure are to enhance load carrying capacity, to reduce deflection at a service loading or to control width and distribution of cracks [1].

Currently, the strengthening of RC structures with fiber reinforced polymer (FRP) is generally conducted by using the externally bonded (EB) FRP technique, which has been widely applied for more than twenty years. Benefits of externally bonded FRP had been widely accepted and had been well documented [2]. The method has become a favorable method of strengthening for owners and construction specialists.

In addition to the EB FRP technique, strengthening by near-surface mounted (NSM) FRP has recently gained popularity as a method for increasing flexural as well as shear capacity of a deficient RC member. The NSM FRP technique for strengthening concrete structures has been used since 1948 and was recently applied to strengthen an RC bridge in Sweden to increase its load carrying capacity [3].

Many studies on the use of NSM FRP for shear strengthening of RC beams without stirrup have been published. Barros and Dias [4] studied the effectiveness of both EB FRP and NSM FRP techniques for shear strengthening of RC members (all beams had no internal stirrups). They reported that the NSM FRP technique was the most effective system in their study. It could increase the load carrying capacity up to 46% in comparison with the EB FRP technique. Rizzo and Lorenzis [5] tested rectangular beams with both stirrups and NSM FRP rods. One strengthened beam failed by peeling-off laterally in the strengthening zone and shear strength increased by 44%. Lorenzis and Nanni [6] carried out tests on eight T-beams (six beams had no stirrup). The NSM FRP technique could increase shear strength as high as 106% of a control beam.

Despite the above studies, information of behaviors and the design for shear strengthening of RC beam with NSM FRP rod is still limited. There is still no standard guideline for NSM strengthening for real practice, especially, that for RC beams with stirrups. Therefore, more tests are necessary to verify the behavior and failure mode of RC beam with stirrups after strengthening with NSM FRP rod.

This article mainly focuses on effects of the NSM FRP technique on the shear behavior in strengthened RC beams with stirrups. The direct pull-out test was tested before conducting tests on beams. The objective of the pull-out test was to compare the suitability groove of sizes (1.5 and 2.0 of rod diameter) for the NSM FRP technique. All beams had stirrups to reproduce an RC element in the real structure. Varied test parameters were types of FRP rod, namely, aramid and carbon fiber reinforced polymer (AFRP and CFRP), spacing and slope of strengthening FRP rods. Finally, existing formulations for NSM FRP shear strengthening proposed by Anwarul [7], Parretti and Nanni [8] and Lorenzis and Nanni [6] were compared with experimental results.

2. Materials

The same materials were used in both the direct pull-out test and the beam test. The compressive strength was evaluated at 28 days and at age of beam tests, carrying out direct compression tests with cylinders of 150 mm diameter and 300 mm height, according to ASTM C39 [9]. The longitudinal and shear reinforcement were a deformed bar of 20 mm (DB20) and a round bar of 6 mm (RB6), respectively. The steel bars were also tested in laboratory according to ASTM A370 standards [10] as shown in Table 1. The mechanical properties of epoxy adhesive in this study are shown in Table 2. The properties of FRP rods used in this study are shown in Table 3.

Table 1 Properties of steel bars.

Properties	DB20	RB6
Yielding strength (MPa)	477	367
Tensile strength (MPa)	643	470

Table 2 Mechanical properties of epoxy adhesive.

Properties	
Tensile strength (MPa)	24
Compressive strength (MPa)	2,750
Slant shear strength (MPa)	34
Elongation at break (%)	0.7

Table 3 Properties of FRP rods provided by the manufacturer.

Properties	AFRP	CFRP
Nominal diameter (d_b) (mm)	13.7	8
Section area (mm^2)	147	47.1
Unit weight (g/m)	173	70
Tensile strength (MPa)	1,100	2,500
Young's modulus (GPa)	68.6	72.4
Elongation at fracture (mm/mm)	1.6	1.3

3. Direct Pull-out Test

3.1 Specimens

Bonding is important since it is the transfer of stress between the concrete and the FRP rods in order to develop composite action. Four specimens were tested to determine the suitable groove size for using in an NSM application by considering three following items:

- (1) The maximum bond strength between concrete and epoxy adhesive as indicated in Table 4.
- (2) The relationship between bond stress and slip at the load end (Fig. 3)
- (3) The amount of epoxy adhesive material

Four specimens were tested to compare two groove sizes; i.e., 1.5 and 2.0 times of rod diameter ($1.5d_b$ and $2.0d_b$) and types of FRP rods. The square groove was used ($b_g = h_g$, b_g and h_g are width and depth of groove, respectively). The dimension of concrete block is shown in Fig. 1. Bond lengths of all specimens were 100 mm. Test results were used to select a groove size for the beam test by considering both limit-state bond failure and maximum bond strength.

Table 4 Bond test specimens and results.

Specimen code*	Groove size	Maximum bond strength (MPa)
1.5A	$1.5d_b$	5.3
1.5C	$1.5d_b$	7.2
2.0A	$2.0d_b$	4.5
2.0C	$2.0d_b$	5.6

*A: AFRP; C: CFRP

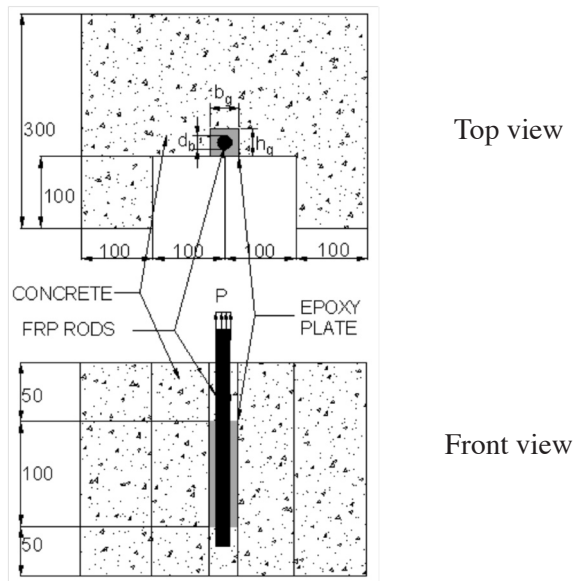


Fig. 1. Direct pull-out test specimen (unit: mm).

3.2 Test set up

Two linear variable differential transducers (LVDTs) were used to record the slip at the loading end. The loading end at top of concrete specimen is shown in Fig. 2. Testing was conducted in displacement-control mode until failure. A typical specimen with the instrumentation is shown in Fig. 2.

3.3 Results and discussion

Table 4 indicates maximum bond strength between concrete and epoxy adhesive material (τ_b) which was computed as follows:

$$\tau_b = \frac{T_u}{\pi \cdot d_b \cdot l} \quad (1)$$

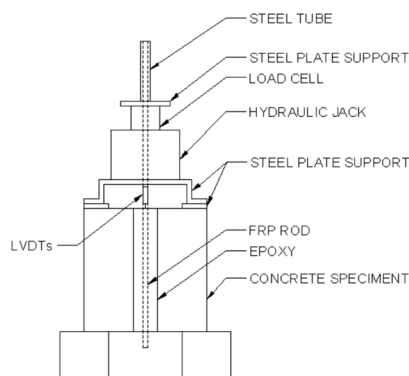


Fig. 2. Test specimen in bond test set up

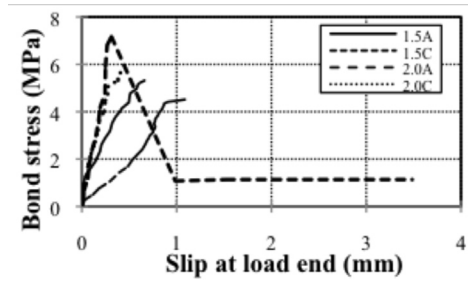


Fig. 3. Bond-slip relationship at the load end of FRP rods.

For specimens 2.0A and 2.0C, the maximum bond strength decreased 15% and 22% as the groove size increased from $1.5d_b$ to $2.0d_b$. With smaller groove size, the thickness of the epoxy cover and the interface area between epoxy and concrete was also smaller. The induced tensile stresses were thus reduced. The the bond mechanism has been previously described by Lorenzis and Nanni [6, 11].

Fig. 3 illustrates that groove size of $1.5d_b$ was stiffer than groove size $2.0d_b$ and the amount of epoxy adhesive used for groove size $1.5d_b$ was less than that for $2.0d_b$. According to this result, the groove size $1.5d_b$ was thus selected for shear strengthening of the beam specimens.

4. Shear behaviors of NSM FRP strengthened RC beam

4.1 Specimens

Seven beams (one control beam and six beams strengthened with NSM FRP rods) were tested to evaluate the efficiency of NSM FRP rods in shear strengthening in the case that stirrups exist (Fig. 4). Overall width and height of cross section were 250 and 300 mm, respectively. The concrete cover thickness from rebar surface to lateral surfaces (four sides of all beams as shown in Fig. 4) was 30 mm. The detail of reinforcement is shown in Fig. 4 and Table 5. The shear strengthening was done by the NSM FRP technique to the both lateral surfaces of the beam and groove size was set at $1.5d_b$. The beams were designed to fail in shear failure mode.

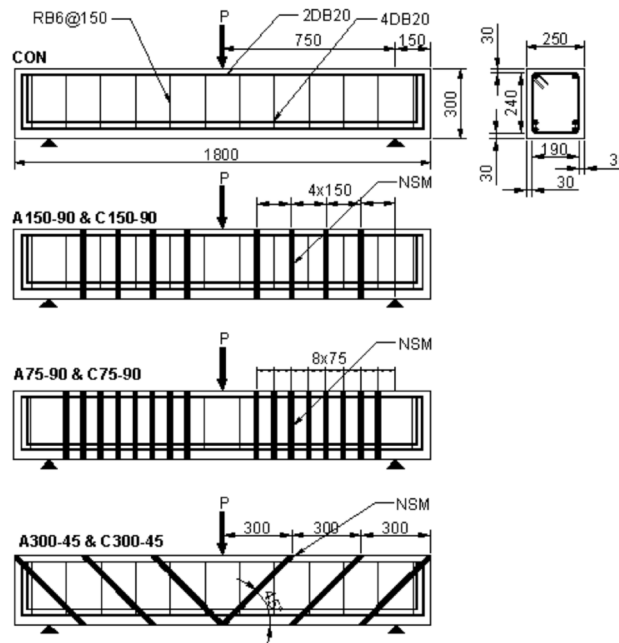


Fig. 4. Beam specimens (unit: mm).

Table 5 Test specimens.

Code	Shear strengthening system	Spacing of steel stirrup (mm)	Spacing of NSM rods (mm)	Slope of NSM FRP (degree)
CON	Steel stirrups	150	-	-
A75-90	Steel stirrups & AFRP	150	75	90
A150-90	Steel stirrups & AFRP	150	150	90
A300-45	Steel stirrups & AFRP	150	300	45
C75-90	Steel stirrups & CFRP	150	75	90
C150-90	Steel stirrups & CFRP	150	150	90
C300-45	Steel stirrups & CFRP	150	300	45

4.2 Test set up

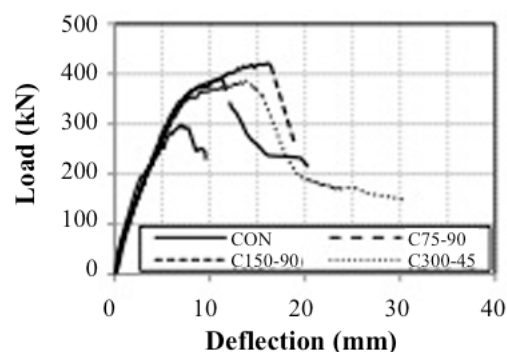
All beams were loaded under three-point loading with a shear span of 750 mm. Total clear span length was 1500 mm as shown in Fig.4. The shear span ratio (a/d) was 3.27.

During loading, data acquisition (DAQ) equipment was used to collect and transfer data to a spreadsheet for analysis. A load cell was used to measure load during testing. Specimens were equipped with four LVDTs (two at mid-span and one at each support) to measure deflection. Load was applied by a manual hydraulic jack.

4.3 Results and discussion

The test results of all beams are summarized in Table 6. P_{max_C} is the ultimate load of a control beam, P_{max_F} is the ultimate load of strengthened beams, the ratio P_{max_F} / P_{max_C} is calculated to assess the efficacy of the shear strengthening of NSM FRP technique in term of the increased load carrying capacity. δ_{max} represents the deflection of the beam at ultimate load. The deformation capacity was evaluated as the ratio $\delta_{max_F} / \delta_{max_C}$.

Fig. 5 and Fig. 6 illustrate the relationship between the load and deflection at mid span. Ultimate load capacities of C75-90, A75-90 and C150-90 were approximately 390kN and all of specimens failed by shear and peeling of NSM layers. A150-90 failed by flexure. This indicates that its shear capacity was more than the flexural capacity (420kN).


Fig. 5. Load-deflection relationship of beams strengthened with AFRP rods.

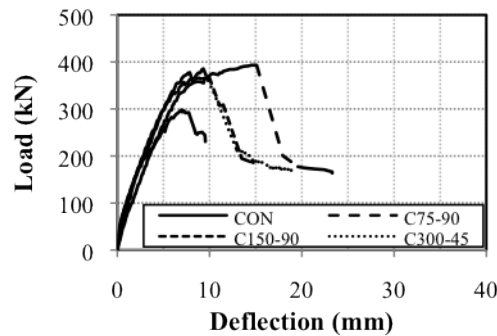


Fig. 6. Load-deflection relationship of beams strengthened with CFRP rods.

Table 6 shows the mid span deflection at ultimate load of all beams. The use of AFRP, as well as, CFRP allowed more deflection before failure. The deflection at failure of RC beams strengthened with NSM FRP rods was two times higher than the control beam. In addition, AFRP caused higher deflection than CFRP. AFRP has lower young's modulus and thus higher elongation than CFRP under the same stress.

For specimens with FRP slope of 45 degree and spacing 300 mm in both cases of AFRP and CFRP (A300-45 and C300-45), the ultimate load was close to specimens with angle 90 degree and spacing of 150 mm (A150-90 and C150-90). Changing the slope of FRP rod to 45 degree (perpendicular to shear cracks) while reducing number of NSM FRP rods is efficient in the NSM FRP technique because the total effective length at NSM FRP rods is increased, and the contribution of each FRP rod to the shear capacity can be consequently increased.

Peeling-off of NSM layer is the separation of strengthening layer (strengthening zone) from inner portion by peeling-off (Fig. 7(b), Fig. 7(e), Fig. 8(a) and Fig. 8(b)) which limits the performance of the NSM FRP technique. Even though the number of NSM rods is increased, the ultimate load may not increase if peeling takes place.

Table 6 Results of experiment.

Code	P_{max} (kN)	$\frac{P_{max,F}}{P_{max,C}}$	δ_{max} (mm)	$\frac{\delta_{max,F}}{\delta_{max,C}}$	Failure mode
CON	297.93	1.00	6.96	1.00	Shear
A75-90	388.87	1.31	11.35	1.63	Shear (peeling of NSM layers)
A150-90	420.75	1.41	16.21	2.33	Flexure
A300-45	385.73	1.29	13.84	1.99	Shear
C75-90	392.99	1.32	15.11	2.17	Shear (peeling of NSM layers)
C150-90	385.43	1.29	9.33	1.34	Shear (peeling of NSM layers)
C300-45	365.32	1.23	9.56	1.37	Shear

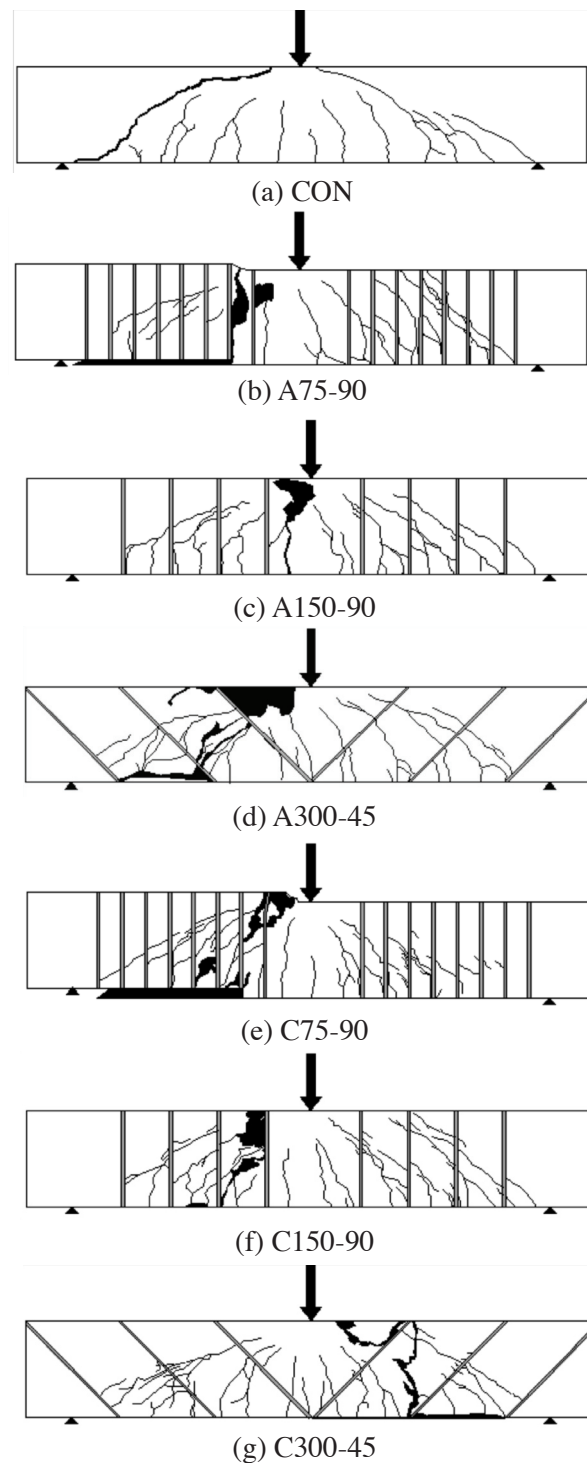
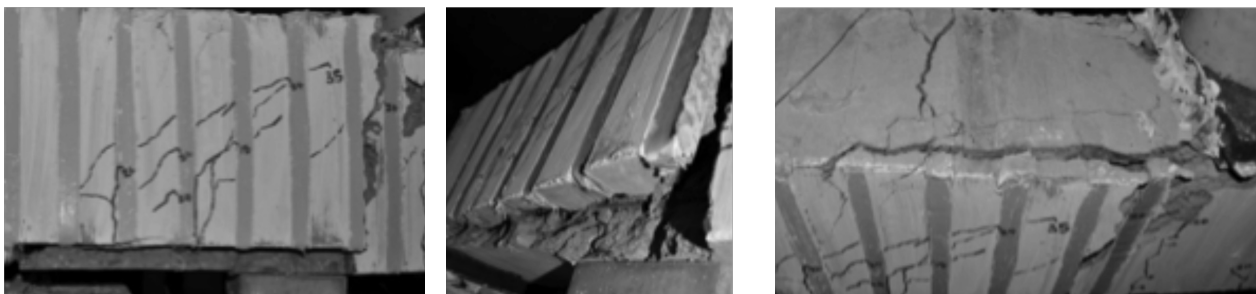


Fig. 7. Beam after shear failure.

Failure modes of A75-90, C75-90 and C150-90 were peeling of NSM layers. The NSM layer in the shear zone had separated from the inner portion and finally the peeling-off portion (NSM layer) was ruptured. On the bottom and top surface of beams, two cracks were found parallel to the lateral face. The distance from a crack to the lateral surface approximately equals the concrete cover thickness. After unloading, the side cover of NSM FRP strengthening surface was removed to observe the conditions of the inner portion. It was found that the diagonal shear crack took place in the inner portion but did not appear on the surface.



(a) Peeling-off of NSM layer (A75-90)

(b) Example of crack parallel to lateral surface (bottom of beam A75-90)

Fig. 8. Failure mode of A75-90.

Crack patterns and failure modes of all beams are shown in Fig. 9. A300-45 and C300-45 failed by shear, and more cracking on the concrete surface between adjacent epoxy-filled grooves took place (Fig. 7(d) and 7(g)). For A300-45 and C300-45, when close to failure, a vertical crack (Fig. 9) started at the bottom of the beam as a flexural-shear crack. The diagonal cracks were not active throughout the entire loading because this was restrained by NSM FRP rods. Similar findings had also been observed in previous experimental programs [12].

5. Shear strength prediction of RC beam strengthened with NSM FRP

With the results of the test on beam strengthened with the NSM FRP technique, the applicability of the currently available formulation proposed by Anwarul [7], Parretti and Nanni [8] and Lorenzis and Nanni [6] were evaluated.

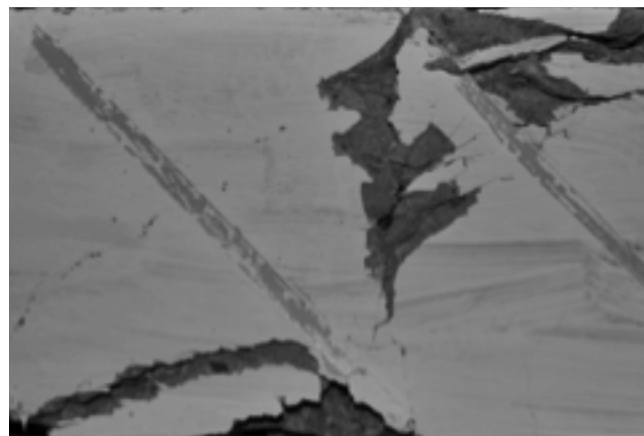


Fig. 9. Crack which propagated through the end of the rod in the beam C300-45.

5.1 Formulation of shear strength

The approach used to calculate the nominal shear capacity of a member strengthened using NSM FRP rods is developed based on ACI440-02 [2] for the case of the EB FRP technique. It is assumed that Eq. (2) is also applicable for the NSM FRP technique and the same strength reduction factor (ϕ) of 0.85 can be used. An additional reduction factor $\psi_f = 0.85$ is applied to the contribution of NSM FRP reinforcement to the shear strength of the member [8]. Thus the nominal shear capacity (V_n) of a RC beam strengthened in shear with NSM FRP rods can be calculated by Eq (2):

$$\phi V_n = \phi(V_c + V_s + \psi_f V_f) \quad (2)$$

Jung and Kim [13] studied many existing design shear formulations by RC beam without stirrup. They concluded that V_c in ACI318-02 building code equation (Eq. (3)) [14] was more conservative than The Okamura equation (Eq. (4)) [15], and the accuracy of the Okamura equation is relatively better than the ACI approach. Therefore, this study selected Okamura-equation to compute shear contribution by concrete (V_c). V_s EMBED Equation.3 is the nominal shear strength provided by steel stirrup and based on expression provided by The ACI318-02 building code, and the code assumes that stirrups yield before failure of specimen (Eq. (5)) [14].

$$V_c = \frac{1}{6} \sqrt{f_c'} b_w d \quad (3)$$

$$V_c = 0.2 \frac{(100\rho)^{1/3}}{(d/100)^{1/4}} (f_c')^{1/3} (0.75 + \frac{1.40}{a/d})^{1/3} b_w d \quad (4)$$

$$V_c = \frac{A_s f_y d}{s} \quad (5)$$

5.2 Formulation by Anwarul [7]

Anwarul [7] developed a formulation with the assumption that that no debonding or no fracture of FRP rod occurs before failure, and the NSM FRP technique works similarly to stirrups. The formulation used 1/3 as factor to reduce the full shear contribution by NSM FRP rods (Eq. (6)), which was set according to the strain of FRP rods at the ultimate state found in his experiment. Anwarul [7] showed that the strain of FRP rod at maximum load was only one-third of the ultimate strain at maximum load in all strengthened beams. Shear contribution from NSM FRP rods at ultimate conditions was thus computed as:

$$V_f = \frac{1}{3} \frac{A_f \cdot f_{fy} \cdot l_{net}}{S_f} \quad (6)$$

$$l_{net} = l_b \cdot \frac{2c}{\sin \alpha} \quad (7)$$

5.3 Formulation by Parretti and Nanni [8]

Parretti and Nanni [8] proposed the calculation of shear contribution from the NSM FRP technique as the force resulting from the tension in FRP rods. The following assumptions are made:

- 1) The slope of the shear cracks is 45 degree.
- 2) bond stresses are constant along the effective length of the FRP rod at ultimate conditions.

Formulation is expressed by Eq. (8)-(12).

$$V_f = 2 \cdot \pi \cdot d_b \cdot \tau_b \cdot L_{tot} \quad (8)$$

L_{tot} is the sum of the effective length of all rod crossed by the crack and can be calculated in Eq. (9).

$$L_{tot} = \sum_i L_i \quad (9)$$

Where, L_i is the length of each NSM FRP rods crossed by a 45 degree shear crack (mm). L_i represents the length of each NSM FRP rods (mm) crossed by a 45-degree shear crack express as follows:

$$L_i = \begin{cases} \frac{s_f}{\cos \alpha + \sin \alpha} \quad i \leq \bar{L}_i, & i = 1 \dots \frac{N}{2} \\ l_{net} - \frac{s_f}{\cos \alpha + \sin \alpha} \quad i \leq \bar{L}_i, & i = 1 \dots \frac{N}{2} + 1 \dots N \end{cases} \quad (10)$$

Where, L_i represents the net length of a FRP rod as shown in Fig. 9 to account for cracking of the concrete cover and installation tolerances (Eq. (11)) and EMBED Equation.3 is the number of FRP rods intercepted by a shear crack as a function (Eq. (12)).

$$\bar{L}_i = 0.001 \frac{d_b E_b}{\tau_b} \quad (11)$$

$$N = \frac{l_{net}(1+\cot\alpha)}{s_f} \quad (12)$$

5.4 Formulation by Lorenzis and Nanni [6]

In the article of Lorenzis and Nanni [6], shear contribution by FRP rods were computed using the same assumptions of Parretti and Nanni [8].

The design approach includes two equations that may be used to obtain V_f . The first equation computes the NSM FRP shear strength contribution related to bond-controlled shear failure as show in Eq. (13).

$$V_f = 2 \cdot \pi \cdot d_b \cdot \tau_b \cdot L_{tot \min} \quad (13)$$

$L_{tot \min}$ is the effective length of all rods crossed by cracks and depends on l_{net} and the spacing of rods. It can be calculated as follows:

$$\text{If } \frac{l_{net}}{3} < s_f < l_{net} \text{ then} \quad (14)$$

$$L_{tot \min} = l_{net} - s_f$$

$$\text{If } \frac{l_{net}}{4} < s_f < \frac{l_{net}}{3} \text{ then} \quad (15)$$

$$L_{tot \min} = 2 \cdot l_{net} - 4 \cdot s_f$$

The second equation calculates the shear resisted by NSM FRP rods when the maximum strain in the rods is equal to $4,000 \mu\epsilon$ which can be calculated by:

$$\text{When, } \frac{l_{net}}{2} < s_f < l_{net};$$

$$V_f = 2 \cdot \pi \cdot d_b \cdot \tau_b \cdot \bar{L}_i \quad (16)$$

When, \bar{L}_i can be obtained in Eq. (11),

When, $\frac{l_{net}}{3} < s_f < \frac{l_{net}}{2}$;

If $l_{net} - 2s_f < \bar{L}_i < s_f$

$$V_f = 2 \cdot \pi \cdot d_b \cdot \tau_b \cdot (\bar{L}_i + l_{net} - 2s_f) \quad (17)$$

If $\bar{L}_i < l_{net} - 2s_f$

$$V_f = 4 \cdot \pi \cdot d_b \cdot \tau_b \cdot \bar{L}_i \quad (18)$$

When, $\frac{l_{net}}{4} < s_f < \frac{l_{net}}{3}$;

If $s_f < \bar{L}_i < l_{net} - 2s_f$

$$V_f = 2 \cdot \pi \cdot d_b \cdot \tau_b \cdot (\bar{L}_i + l_{net} - 2s_f) \quad (19)$$

If $l_{net} - 3s_f < \bar{L}_i < s_f$

$$V_f = 2 \cdot \pi \cdot d_b \cdot \tau_b \cdot (\bar{L}_i + l_{net} - 3s_f) \quad (20)$$

If $\bar{L}_i < l_{net} - 3s_f$

$$V_f = 6 \cdot \pi \cdot d_b \cdot \tau_b \cdot \bar{L}_i \quad (21)$$

5.5 Examination of existing models

Based on material properties and dimension of the beam specimen, the nominal shear capacity was calculated. It was assumed that stirrups yielded at failure for all specimens. The analysis results showed that all existing formulations can be used to predict shear capacity of beam with NSM FRP within an accuracy of 3%-10% of the experimental value except the case of A75-90 and C75-90 where peeling-off took place. This article makes the comparison between experimental behavior strengthen beams and the existing formulation as shown in Fig. 10.

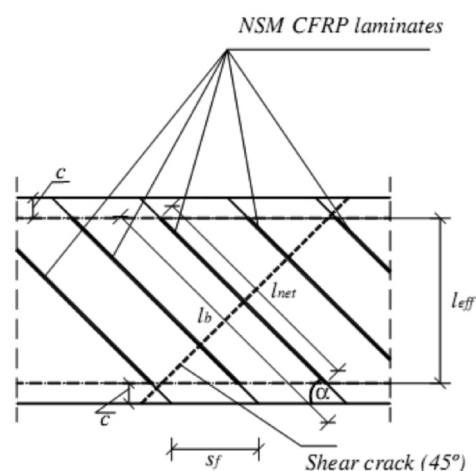


Fig. 10. Graphical representation of variables used in the formulation proposed by Parretti and Nanni [8].

Fig.11 compares nominal shear capacities calculated from each existing model with experimental results. All formulations could not give accurate shear capacities of beams that failed by peeling-off of an NSM layer. The values calculated from all existing formulations were much higher than the experimental results in cases that peeling-off took place.

The discrepancy found in the case of A75-90, C75-90 may be because no consideration of peeling-off has been taken into account in any existing formulations. All formulations provide no warning signs on the possibility of peeling-off when too many rods are installed. The criteria to prevent peeling-off failure should thus be incorporated in the formulation of NSM FRP shear strengthening in the future.

Further study is needed formulation for using to predict the shear capacity of strengthening beam with NSM FRP rods in cases of peeling-off.

6. Conclusions

The following conclusions from this study can be drawn:

- Groove size of $1.5d_b$ for NSM application is more effective in three ways; more bond between concrete and epoxy adhesive, more stiffness, and less amount of epoxy adhesive needed (when compared with the case of $2.0d_b$)
- NSM FRP strengthening has a high potential to increase shear capacity of RC beams. Shear capacity of strengthened beam can be increased in the range of 23%-41% compared to a control beam. In the case of peeling-off failure mode, the minimum shear capacity of a strengthened beam increases approximately 30%.
- Peeling-off of an NSM layer, once it takes place, limits the efficiency of a shear strengthening beam by the NSM FRP technique.
- Although adding more number of FRP rods generally increases shear capacity, this may lead to peeling-off of an NSM layer if the spacing of NSM FRP rods or concrete cover is too small.
- All existing formulations cannot be used to predict shear capacity in the case of beams that failed by peeling-off of an NSM layer.

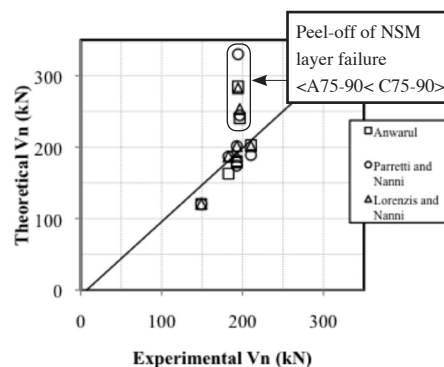


Fig. 11. Comparison of experimental and theoretical V_n .

7. Acknowledgements

The authors are very grateful to National Science and Technology Development Agency (NSTDA) for providing the research fund No. PS0900307/P-09-00080 and to BASF (Thailand) Co., Ltd for materials used in this experimental work.

8. References

- [1] Hollaway M.A. and Raouf M., Strengthening of Reinforced Concrete Structure: CRC press, 2001.
- [2] ACI Committee 440, Guide for the Design and Construction of Externally Bonded FRP System for Strengthening Concrete Structures, ACI, Farmington Hills, Michigan, 2002.
- [3] Asplund S. O., Strengthening Bridge Slabs with Grouted Reinforcement, ACI Structural J., 1949.
- [4] Barros J. A. O. and Dias S. J. E., Near Surface Mounted CFRP Laminates for Shear Strengthening of Concrete Beams, Composite part B 28, pp. 276 - 292, 2006.
- [5] Rizzo A. and Lorenzis L. D., Behavior and Capacity of RC Beams Strengthening in shear with NSM FRP reinforcement, Construction and Building Material 23, pp 1555 - 1567, 2009.
- [6] Lorenzis L. D. and Nanni A., Near Strengthening of Reinforced Concrete Beams with Near-Surface Mounted Fiber-Reinforced Polymer Rods, ACI Structure J., Title No. 98 - S6, pp. 60 - 68, 2001.
- [7] Anwarul Islam A. K. M., Effective Methods of Using CFRP Bars in Shear Strengthening of Concrete Girders, Engineering Structures 21, pp. 709 - 714. 2008.
- [8] Parretti R. and Nanni A., Strengthening of RC Members Using Near-Surface Mounted FRP Composites: Design Overview, Advances in Structural Engineering Vol. 7, No. 5, 2004.
- [9] ASTM C39, Standard Test Methods for Compressive Strength of Cylindrical Concrete Specimens, American Society for Testing and Materials, West Conshohocken, PA, 2005.
- [10] ASTM A370, Standard Test Methods and Definitions for Mechanical Testing of Steel Products, American Society for Testing and Materials, West Conshohocken, PA, 2005.
- [11] Lorenzis L. D. and Nanni A., Characterization of FRP Rods as Near-Surface Mounted Reinforcement. Journal of Composites for Construction, pp. 114 - 121, 2001.
- [12] Dias S. J. E. and Barros J. A. O., Performance of Reinforced Concrete T Beams Strengthened in Shear with NSM CFRP Laminates, Engineering Structures 32, pp. 373 - 384, 2010.
- [13] Jung S. and Kim. K. S., Knowledge-Based Prediction of Shear Strength of Concrete Beams without Shear Reinforcement, Engineering Structures 30, pp. 1515 - 1525, 2008.
- [14] ACI Committee 318, ACI Building Code Requirements for Reinforced Concrete, ACI, Detroit, Michigan, 1995.
- [15] Okamura H. and Higai T., Propose design Equation for Shear Strength of Reinforcement Concrete Beams without Web Reinforcement. Proc. of JSCE 300, pp. 131 - 141, 1980.

9. Notations

α	=	slope of the FRP rod with respect to the beam longitudinal axis (degree)
τ_b	=	average bond strength between concrete and epoxy adhesive material (MPa)
$\bar{\phi}$	=	strength reduction factor
ψ_f	=	additional reduction factor
a	=	shear span (mm)

A_f	=	cross section area of FRP rod (mm ²)
A_s	=	cross sectional area of steel (mm ²)
b_w	=	width of concrete web (mm)
c	=	concrete clear cover (mm)
d	=	effective depth (mm)
d_b	=	nominal rod diameter (mm)
E_b	=	elastic modulus of a FRP rod (MPa)
f'_c	=	concrete compressive strength (MPa)
f_{fs}	=	tensile strength of FRP rod (MPa)
f_{fy}	=	yielding strength of stirrup (MPa)
l	=	bond length (mm)
l_b	=	actual length of a FRP rod (mm)
l_{net}	=	net length of a FRP rod (mm)
L_i	=	length of each NSM FRP rods crossed by 45 degrees (mm)
L_i	=	net length of a FRP rod (mm)
L_{tot}	=	effective length of all rod crossed by the crack (mm)
$L_{tot\ min}$	=	effective length of all rod crossed by crack (mm)
N	=	number of FRP rod intercepted by a shear crack
p_l	=	longitudinal reinforcement ratio
s	=	spacing of stirrup (mm)
s_f	=	spacing of NSM FRP rod (mm)
T_u	=	ultimate tensile load (kN)
V_c	=	shear strength provided by concrete (kN)
V_f	=	shear contribution by FRP rod (kN)
V_n	=	nominal shear capacity (kN)
V_s	=	shear strength provided (kN)